Journal of Medicinal Chemistry

ARTICLE

pubs.acs.org/jmc

Leucettines, a Class of Potent Inhibitors of cdc2-Like Kinases and Dual Specificity, Tyrosine Phosphorylation Regulated Kinases Derived from the Marine Sponge Leucettamine B: Modulation of Alternative Pre-RNA Splicing

Mansour Debdab,[†] François Carreaux,[*,†] Steven Renault,[†] Meera Soundararajan,[‡] Oleg Fedorov,[‡] Panagis Filippakopoulos,[‡] Olivier Lozach,[§] Lucie Babault,[§] Tania Tahtouh,[§] Blandine Baratte,[§] Yasushi Ogawa,[∥] Masatoshi Hagiwara,[⊥] Andreas Eisenreich,[#] Ursula Rauch,[#] Stefan Knapp,[‡] Laurent Meijer,[*,§] and Jean-Pierre Bazureau[*,†]

[†]Université de Rennes 1, Sciences Chimiques de Rennes, UMR CNRS 6226, Groupe 'Ingénierie Chimique & Molécules pour le Vivant' (ICMV), Bât. 10A, Campus de Beaulieu, Avenue du Général Leclerc, CS 74205, 35042 Rennes cedex, France

[‡]Nuffield Department of Clinical Medicine, Structural Genomics Consortium, Oxford University, Old Road Campus Research Building, Headington, Oxford OX3 7DQ, U.K.

[§]Station Biologique de Roscoff, CNRS, 'Protein Phosphorylation and Human Disease' Group, Place G. Teissier, BP 74, 29682 Roscoff, France

[∥]Department of Dermatology, Nagoya University Graduate School of Medicine, 65 Tsurumai-cho, Showa-ku, Nagoya 466-8550, Japan

[⊥]Department of Anatomy and Developmental Biology, Graduate School of Medicine, Kyoto University, Yoshida-Konoe-cho, Sakyo-ku, Kyoto 606-8501, Japan

[#]Charité-Universitätsmedizin-Berlin, Campus B. Franklin, Centrum für Herz- und Kreislaufmedizin, Hindenburgdamm 30, 12203 Berlin, Germany

Supporting Information

ABSTRACT: We here report on the synthesis, optimization, and biological characterization of leucettines, a family of kinase inhibitors derived from the marine sponge leucettamine B. Stepwise synthesis of analogues starting from the natural structure, guided by activity testing on eight purified kinases, led to highly potent inhibitors of CLKs and DYRKs, two families of kinases involved in alternative pre-mRNA splicing and Alzheimer's disease/Down syndrome. Leucettine **L41** was cocrystallized with CLK3. It interacts with key residues located within the ATP-binding pocket of the kinase. Leucettine **L41** inhibits the phosphorylation of serine/arginine-rich proteins (SRp), a family of proteins regulating pre-RNA splicing. Indeed leucettine **L41** was demonstrated to modulate alternative pre-mRNA splicing, in a cell-based reporting system. Leucettines should be further explored as pharmacological tools to study and modulate pre-RNA splicing. Leucettines may also be investigated as potential therapeutic drugs in Alzheimer's disease (AD) and in diseases involving abnormal pre-mRNA splicing.

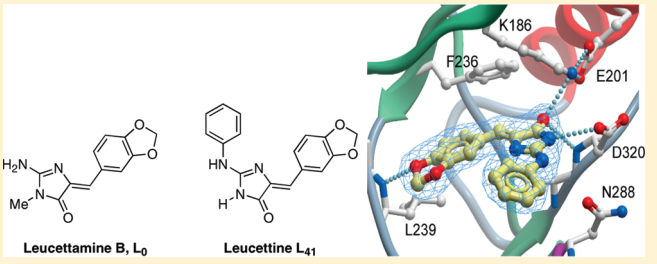

INTRODUCTION

Marine organisms constitute a rich source of high diversity chemical structures.[1] Marine natural products are being explored for multiple biomedical applications, mostly as potential anticancer agents but also in other therapeutic indications such as inflammation, neurodegenerative diseases, parasites, viral infections, and renal pathologies.[2] Among the many marine natural products that have been isolated, a number of molecules share a 2-aminoimidazolone ring structure (Figure 1). The best studied molecules of this series include leucettamine B,[3,4] polyandrocarpamines,[5] dispacamide,[6] aplysinopsine,[7] and hymenialdisine.[8] The marine sponge alkaloid (*Z*)-hymenialdisine was found to be a nanomolar inhibitor of various protein kinases including glycogen synthase-3β (GSK-3 β), casein kinase 1 (CK1), and different cyclin-dependent kinases (CDKs),[9] mitogen-activated protein kinase 1 (MEK-1),[10] and checkpoint kinase 1.[11] Protein kinases are the enzymes which catalyze protein phosphorylation, a key cellular regulatory mechanism which is frequently deregulated in human diseases. Consequently, protein kinases represent interesting

Received: March 9, 2011
Published: May 26, 2011

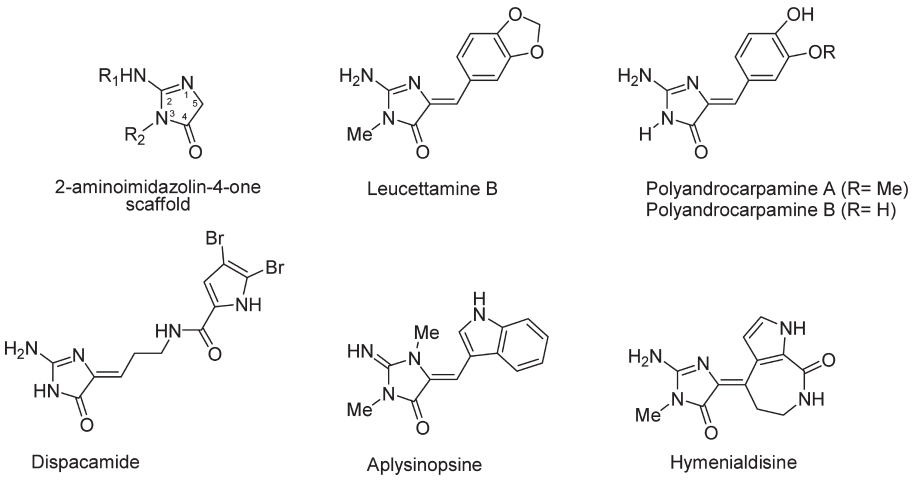

Figure 1. Selection of marine organism-derived structures sharing the 2-aminoimidazolone ring structure.

targets for the pharmaceutical industry in its search for new therapeutic agents. In our efforts to discover new low molecular weight inhibitors of disease-relevant protein kinases, we focused our attention on leucettamine B (Figure 1). This natural compound was isolated in 1993 from the sponge *Leucetta microraphis* Haeckel (*Calcarea*) of the Argulpelu Reef in Palau,[3] and to date, no significant biological activity of this compound has been reported. From a preliminary biological screening of this natural product, we found that leucettamine B exerted a selective inhibition toward protein kinases that are potential targets for the treatment of Alzheimer's disease. Several methods for the synthesis of leucettamine B and analogues have been developed.[12] In this article, we report on the synthesis of leucettines, a family of derivatives of leucettamine B, guided by their inhibitory action on a panel of eight protein kinases. A detailed structure−activity relationship (SAR) led to the identification of the first potent inhibitors of two families of serine/threonine kinases, dual-specificity, tyrosine phosphorylation regulated kinases (DYRKs), and cdc2-like kinases (CLKs), which are involved in Alzheimer's disease/Down syndrome and in the control of alternative pre-mRNA splicing. We also report on a cocrystal structure of a leucettine with CLK3. Using two different cellular models, we demonstrate that leucettine modulates alternative pre-mRNA splicing, most probably through phosphorylation of serine/arginine-rich proteins (SRp). Altogether, the presented data should provide the basis for the design and optimization of selective inhibitors, on the basis of the leucettine scaffold, for key protein kinases involved in the regulation of pre-mRNA splicing[13] and development of Alzheimer's disease,[14] Down syndrome,[15] and other severe central nervous system pathologies.

RESULTS AND DISCUSSION

In our screening efforts to discover new scaffolds for the inhibition of disease-relevant protein kinases, we initially screened a library of over 45,000 low molecular weight compounds on the kinase DYRK1A (dual-specificity, tyrosine phosphorylation activated kinase 1A).[14,15] This library comprised numerous natural products including molecules bearing a 2-aminoimidazolone ring. Among these, the marine-sponge-produced leucettamine B was found to be a modest but significant inhibitor of this Alzheimer's disease[14] and Down syndrome[15]-relevant kinase. We next set up a method to synthesize leucettamine B in order to obtain a sufficient quantity of this natural product for more advanced biological evaluations (Scheme 1). The synthetic leucettamine B $\mathbf{L_0}$ was thus tested on a small panel of eight kinases, most of which are involved in Alzheimer's disease (Table 1). Leucettamine B displayed an IC_{50} value in the submicromolar/micromolar range for DYRK1A, DYRK2, CLK1, and CLK3 but was inactive on GSK-3α/β, CK1δ/ε, CDK5/p25, and Pim1. A more detailed study of the selectivity of leucettamine B will be presented elsewhere (manuscript in preparation).

Development of Efficient Synthetic Routes. To access derivatives of leucettamine B (referred to as leucettines), we established a number of synthetic routes. Leucettamine B, $\mathbf{L_0}$ was prepared in three steps starting from commercially available methylisothiocyanate and methyl glycinate hydrochloride as depicted in Scheme 1.[16] For the synthesis of analogues with wide substitution diversity at the 2-amino position, we selected three different routes as shown in Scheme 1. Introduction of acyl groups at this position was achieved by treating the natural product, $\mathbf{L_0}$ with acyl chlorides in the presence of triethylamine under standard literature conditions. Compounds were obtained after purification by chromatography on silica gel.

The synthesis of *N*-monoalkyl substituted analogues was carried out by the simple conversion of (*Z*)-thiohydantoin **3a** to the corresponding 2-aminoimidazolones using *tert*-butyl hydroperoxide (TBHP) as an oxidant in the presence of primary amines. We obtained moderate to good yields of desired products with some primary alkyl amines. However, we observed that the yield of this reaction is highly dependent on the nature of amines used, rendering this method a route unsuitable for the synthesis of a large library of compounds.

A third synthetic strategy was thus employed in particular for the introduction of aromatic groups or substituents including a reactive group (e.g., −OH or NH_2). This sequence begins by the synthesis of **4a** obtained using a one pot procedure, followed by displacement of the SEt group with amines. For this last reaction, two methods have been developed in order to increase the number of amines which could be used. Treatment of **4a** with an excess of alkylamines at reflux in an oil bath resulted in clean conversion to substitution products. Regarding the sulfur/nitrogen displacement by anilines derivatives, reactions were performed under microwave irradiation without solvent. Using these three

Scheme 1. General Procedure for the Synthesis of Leucettines Substituted at the 2-Amino Position[a]

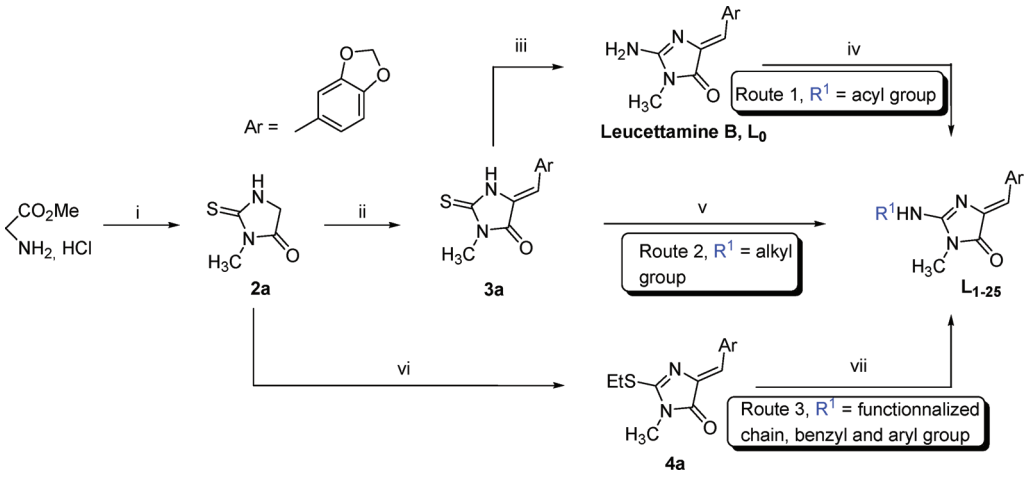

[a] Reagents and conditions: (i) MeN=C=S, Et_3N, Et_2O, reflux, 14 h, 95%; (ii) ArCH=N−Pr, $\mu\omega$ (Synthewave 402 reactor, Prolabo), 80 °C, 1 h, 87%; (iii) TBHP, NH_4OH, CH_3OH, r.t., 48 h, 60%; (iv) R^1COCl, Et_3N, THF, r.t.; (v) R^1NH_2, TBHP, CH_3OH, r.t., 48 h; (vi) EtI, ArCH=N−Pr, CH_3CN, 60 °C, 16 h, 62%; (vii) method A: R^1NH_2, reflux, 3 days; method B: R^1NH_2, $\mu\omega$ (Synthewave 402 reactor, Prolabo), 100−160 °C, 20−100 min.

Table 1. Effects of Leucettamine B on the Catalytic Activity of Eight Purified Protein Kinases[a]

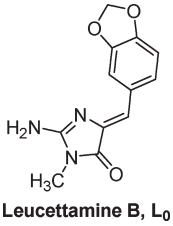

	DYRK1A	DYRK2	CLK1	CLK3	GSK-3α/β	CK1δ/ε	CDK5/p25	Pim1
leucettamine B	2.8	1.5	0.40	6.4	>10	>10	>10	>10

[a] Leucettamine B was tested at various concentrations on DYRK1A, DYRK2, CLK1, CLK3, GSK-3α/β, CK1δ/ε, CDK5/p25, and Pim1 as described in the Experimental Section. IC_{50} values, calculated from the dose−response curves, are reported in μM.

different routes, we have prepared more than 200 molecules from which 25 ($\mathbf{L_{1-25}}$) were selected for our study (Table 2).

In a second approach, we decided to prepare leucettamine B analogues with different aromatic groups at position 5 of the ring. The synthetic route to reach this goal is shown in Scheme 2. S-Alkylation of compound **2a** with methyl iodide, followed by a solvent-free Knoevenagel reaction under microwave conditions with different aldehydes, provided compounds $\mathbf{6a_{1-5}}$ with a well-defined stereochemistry. All compounds were obtained solely as their *Z* isomers, and no isomerization at the exocyclic double bond was subsequently observed. The choice of the amine to realize the substitution of SMe group has been guided by biological results. Finally, $\mathbf{6a_{1-5}}$ were heated in neat propylamine to provide substitution products $\mathbf{L_{26-30}}$ (Table 3).

A similar strategy was used for the synthesis of analogues $\mathbf{L_{31-33}}$ with different substitutions at the 3-amino position of the 2-aminoimidazolin-4-one scaffold (Table 4). This approach using thiohydantoins **2b−d** as starting material was based on a S-alkylation/condensation/substitution sequence as described in Scheme 3. **2b** (R^2 = H) is a commercially available compound and **2c−d** (**2c**, R^2 = *n*-Bu; **2d**, R^2 = Ph) were easily prepared by the reaction of methyl glycinate with the corresponding isothiocyanates, according to the same conditions used for the synthesis of **2a**.

To complete our work on the quantitative structure−activity relationship (QSAR) of leucettines as kinase inhibitors, and taking the biological results obtained with the previous compounds into account (see biological evaluation), we designed synthetic pathways for the preparation of a small library of unsubstituted analogues at the 3-amino position (Scheme 4). From the starting material **2b**, eight products $\mathbf{L_{34-41}}$ (Table 5) were synthesized employing, in the last step, either thermal or microwave conditions for sulfur/nitrogen displacement according to the nature of the used amines.

Leucettines described in this article were typically precipitated by the addition of ethanol or ether and were sufficiently pure for in vitro testing or were purified by silica gel chromatography (see Experimental Section). Structural confirmations of all compounds were performed by extensive 1D and 2D

dx.doi.org/10.1021/jm200274d |*J. Med. Chem.* 2011, 54, 4172–4186

Table 2. Effects of Leucettines L_{1-25} on the Catalytic Activity of Eight Purified Protein Kinases[a]

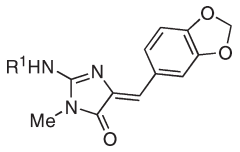

$L_{1\text{-}25}$

Compound	R^1	DYRK 1A	DYRK 2	CLK1	CLK3	GSK-3α/ß	CK1	CDK5/ p25	Pim1
L_1	Me	2.1	2.2	0.77	3.2	18	-	-	3.5
L_2	CH_3CH_2	0.58	0.64	0.17	2.1	16	-	-	7.2
L_3	$CH_3CH_2CH_2$	0.54	0.55	0.31	1.2	3	-	-	4.5
L_4	Me_2CH	0.39	0.53	0.26	2	1.8	-	-	4
L_5	$CH_3CH_2CH_2CH_2$	0.5	0.61	0.13	1.1	3.3	-	-	4.6
L_6	Me_2CHCH_2	0.17	0.21	0.12	0.9	3.1	-	-	2
L_7	$Me_2CHCH_2CH_2$	0.46	0.56	0.16	0.96	2	-	-	2.1
L_8	$H_2C{=}CHCH_2$	0.44	0.62	0.20	0.88	1.6	-	-	4.2
L_9		0.2	0.34	0.13	0.51	0.6	-	> 10	2.1
L_{10}		3.7	6	0.14	> 10	1.7	-	-	0.3
L_{11}	$HOCH_2CH_2$	7	10	0.12	> 10	1.3	-	-	> 10
L_{12}	$MeOCH_2CH_2$	0.57	0.77	0.073	3.1	>100	-	-	> 10
L_{13}	$HOCH_2CH_2CH_2$	0.28	0.47	0.233	3.9	4.5	-	-	6.5
L_{14}	$HOCH_2(CH_2)_3CH_2$	2.1	2	0.14	7	>10	-	-	6.1
L_{15}	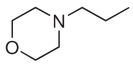	1.2	1.6	0.080	8	4	-	-	6.2
L_{16}	$H_2NCH_2CH_2$	0.91	0.71	0.19	5	0.91	-	-	3.1
L_{17}	MeCO	3.1	5.1	2.4	> 10	>10	-	-	> 10
L_{18}	$EtO_2C\text{-}CO$	6.1	6.5	3.1	> 10	>10	-	-	7
L_{19}	$C_6H_5CH_2$	0.38	0.56	0.20	0.94	>10	-	-	3.7
L_{20}	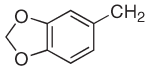	3.2	3.3	0.23	> 10	>10	-	-	0.59
L_{21}	C_6H_5	0.31	0.46	0.084	4.6	4.3	-	-	2.6
L_{22}	$p\text{-}HOC_6H_5$	0.44	1.1	1.0	3.9	1.6	-	-	4.0
L_{23}	$p\text{-}MeOC_6H_5$	0.24	0.51	0.45	> 10	0.7	-	-	4.1
L_{24}	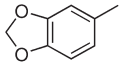	0.4	0.1	0.16	> 10	5.8	-	-	> 10
L_{25}	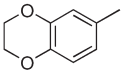	0.22	0.12	0.22	3.6	1.2	-	> 10	2.2

[a] Compounds were tested at various concentrations on each kinase as described in Experimental Section. IC_{50} values are reported in μM. -, inactive at the highest concentration tested (10 μM); >10, inhibitory but IC_{50} >10 μM.

NMR spectroscopy. The geometry about the exocyclic double bonds of L_{0-41} was determined on the basis of $^{13}C/^{1}H$ long-range coupling constants which were measured in a gradient heteronuclear single quantum multiple bond correlation (gHSQMBC) experiment.

dx.doi.org/10.1021/jm200274d |J. Med. Chem. 2011, 54, 4172–4186

Scheme 2. General Procedure for the Introduction of Substituents at Position 5 of the Ring (Corresponding to Table 3)[a]

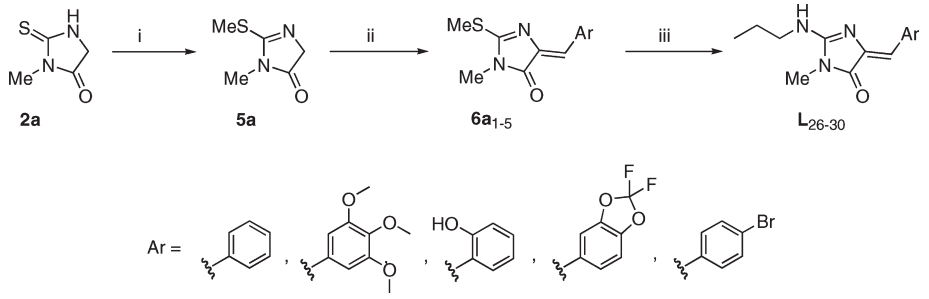

[a] Reagents and conditions: (i) CH_3I, K_2CO_3, CH_3CN, 40 °C, 14 h, 95%; (ii) ArCHO, piperidine, $\mu\omega$ (Synthewave 402 reactor, Prolabo), 70 °C, 15−25 min; (iii) *n*-$PrNH_2$, reflux, 3 days.

Table 3. Effects of Leucettines L_{26-30} on the Catalytic Activity of Eight Purified Kinases[a]

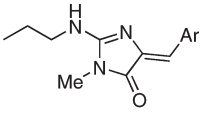

L_{26-30}

Compound	Ar	DYRK 1A	DYRK 2	CLK1	CLK3	GSK-3α/ß	CK1	CDK5/ p25	Pim1
L_3	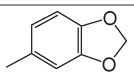	0.54	0.55	0.31	1.2	3	-	-	4.5
L_{26}		-	-	-	-	-	-	-	> 10
L_{27}	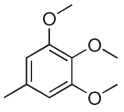	-	> 10	>10	-	-	-	-	> 10
L_{28}	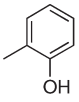	> 10	> 10	>10	> 10	-	-	-	> 10
L_{29}	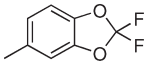	-	-	-	-	-	-	-	> 10
L_{30}	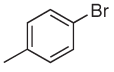	>10	-	-	8.8	-	-	-	-

[a] Compounds were tested at various concentrations on each kinase as described in Experimental Section. IC_{50} values are reported in μM. -, inactive at the highest concentration tested (10 μM); >10, inhibitory but IC_{50} >10 μM.

Biochemical Evaluation of Leucettines and the Cocrystal Structure of Leucettine L_{41} with CLK3. On the basis of the activity of Leucettamine B on DYRKs, CLKs, GSK3 α/β, CK1δ/ε, CDK5/p25, and Pim1 (Table 1), we tested the prepared analogues on a panel of eight kinases.

Table 2 highlights the structures for 25 compounds which were selected from over 200 analogues synthesized in our program. Testing on the kinase panel revealed that, with a few exceptions (L_6, L_{17-18}), leucettines substituted at the 3-amino position showed a similar or increased activity toward all kinases compared to the natural product. These observations indicated that the primary amino group is not essential for the biological activity of leucettamine B. For inhibitors where R^1 was an alkyl group, the highest inhibitory potencies were observed using cyclic chains (L_{9-10}) compared to those of linear or branched chains (L_{1-8}).

To gain insight into the binding mode of leucettines, we determined the crystal structure of compound L_{41} in complex with CLK3. The structure was refined to a 2.09 Å resolution allowing detailed description of the interaction of L_{41} with the

dx.doi.org/10.1021/jm200274d |*J. Med. Chem.* 2011, 54, 4172–4186

Table 4. Effects of Leucettines L_{31-33} on the Catalytic Activity of Eight Purified Kinases[a]

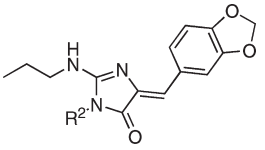

L_{31-33}

compound	R_2	DYRK1A	DYRK2	CLK1	CLK3	GSK-3α/β	CK1	CDK5/p25	Pim1
L_3	CH_3	0.54	0.55	0.31	1.2	3	-	-	4.5
L_{31}	H	0.24	0.12	0.13	2.2	7.3	-	-	2.5
L_{32}	$CH_3CH_2CH_2$	>10	2.1	-	-	-	-	-	>10
L_{33}	C_6H_5	>10	>10	>10	>10	-	-	-	>10

[a] Compounds were tested at various concentrations on each kinase as described in Experimental Section. IC_{50} values are reported in μM. -, inactive at the highest concentration tested (10 μM); >10, inhibitory but IC_{50} >10 μM.

Scheme 3. General Procedure for the Introduction of Substituents at the 3-Amino Position of the 2-Aminoimidazolin-4-one Scaffold[a]

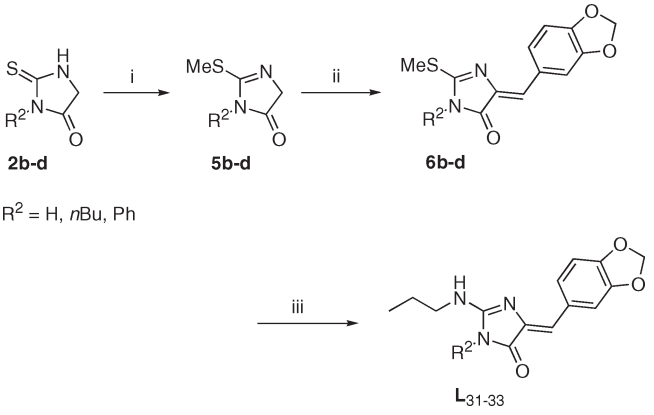

2b-d 5b-d 6b-d

R^2 = H, *n*Bu, Ph

L_{31-33}

[a] Reagents and conditions: (i) CH_3I, K_2CO_3, CH_3CN, 40 °C, 14 h; (ii) piperonal, piperidine, μω (Synthewave 402 reactor, Prolabo), 70 °C, 15−25 min; (iii) *n*$PrNH_2$, reflux, 3 days.

kinase active site. The structure revealed that leucettines interacted with CLK3 as ATP-competitive inhibitors (Figure 2). The 2-amino imidazoline scaffold formed a network of hydrogen bonds with the conserved active site lysine residue (E201) and the DFG motif anchoring the inhibitor in the ATP binding site. The benzodioxole ring formed a hydrogen bond with the main chain amide of the hinge residue L239, and a number of hydrophobic interactions contributed to the binding affinity of this inhibitor.

SAR analysis showed that the presence of a hydroxyl group in the alkyl chain selectively enhanced the activity toward DYRK1A and CLK1 compared to that of GSK-3α/β. The slightly increased affinities of compounds L_{11} and L_{13-14} could result from a favorable electrostatic interaction between the oxygen atom and the binding cavity in DYRK1A and CLK1 kinases, possibly due to hydrogen bond accepting. This is particularly evident for compound L_{12} which contained a protected hydroxyl group. In contrast, a primary amino function at the end of the alkyl chain was favorable for GSK-3α/β inhibition (L_{16}). Introduction of an acyl side chain on the amino group generally reduces activity (L_{17-18}). This lack of affinity might be explained by a reduction of the hydrogen bond potential of an amide function compared to that of a secondary amino group.

From these results, it thus appears that the presence of an aromatic substitution on the amino group has a beneficial effect on the activity toward these kinases. In particular, a ring system containing a protected hydroxyl group selectively appears to favor inhibition of DYRK1A and CLK1. This hypothesis was tested by preparing compounds L_{19-25}. We found that aryl groups had better potency than benzyl groups for DYRK1A and CLK1 (L_{19} compared to L_{21}). Results obtained with L_{22} confirmed the additional beneficial effect of an aromatic group and of a hydroxyl group in para position at the aromatic ring.

We next modified the 2-aminoimidazolin-4-one scaffold at position 5, keeping a propyl group at the 2-amino position (Table 3). Despite the diversity of aromatic ring substitutions, only the 1,3-benzodioxole substituent was able to maintain some inhibitory activity toward the kinases. This observation can be explained by our structural data of the L_{41} /CLK3 complex which suggested that the presence of an oxygen atom at the benzodioxole moiety is necessary for interaction with the hinge backbone and hence for inhibitor potency. The presence of bulky methyl groups on the phenyl group (L_{27}) instead of the nearly planar 5-membered methylenedioxy ring is likely to create clashes with the hinge region, rendering this substitution unfavorable for affinity. The inherent flexibility of the methoxy groups probably reduces ligand stabilization and anchoring.

Even a minor modification of this group such as the replacement of hydrogen atoms (L_3) by fluorine atoms (L_{29}) abolished biochemical activity. The analogue L_{29} is a non-binder probably because of the perturbation of the electron distribution of the ring. Initial b3lyp/DFT calculations show that in L_{29} the partial charge of both oxygen atoms is less negative (approximately up to 0.1e), and the charge of the fluorine atoms is more positive (approximately up to 0.5e). This most likely causes electrostatic repulsion between such inhibitors and the kinase hinge region (e.g., the backbone carbonyl function of Leu241) or increases the desolvatation penalty for this compound.

Keeping a propyl-amino group at position 2 and 1,3-benzodioxole residue at position 5, we next studied the effects of modifications on the nitrogen atom at position 3 (Table 4). The

dx.doi.org/10.1021/jm200274d |J. Med. Chem. 2011, 54, 4172–4186

conversion of N-Me to NH group ($\mathbf{L_3}$ compared to $\mathbf{L_{31}}$) favors affinity for DYRK1A moderately (4 fold improvement). For CLK1 and GSK-3α/β, we observed variations in affinity potency in both directions but still moderately (2-fold improvement for CLK1 and 3-fold decrease for GSK-3α/β). However, the lack of a clear trend in SAR suggests that there might possibly be different binding modes to these kinases. However, it is clear that replacement of the methyl group by a hydrogen atom enhances the inhibitory activity toward DYRK1A and CLK1 versus GSK3α/β (Table 4), raising the possibility that selective inhibitors of DYRK1A/CLK1 can be designed.

We next carried out modifications on the exocyclic nitrogen atom from the scaffold bearing a hydrogen atom on N-3. Following evaluation on the kinase panel (Table 5), it appears that the absence of a substituent on the nitrogen atom N-3 associated with the presence of an aromatic nucleus on the exocyclic amine

Scheme 4. General Procedure for the Synthesis of Leucettines Unsubstituted at the 3-Amino Position of the Ring[a]

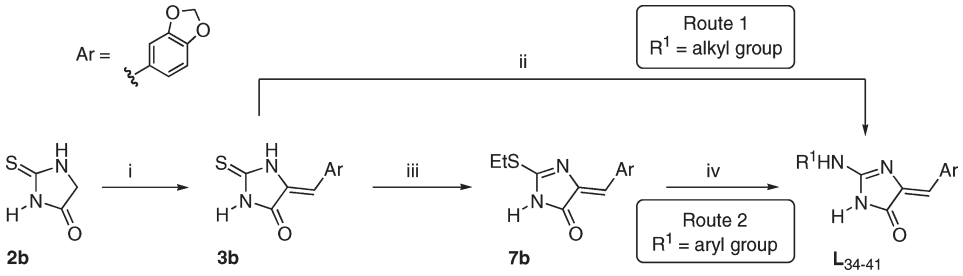

[a] Reagents and conditions: (i) ArCH=N−Pr, CH_3CN, 80 °C, 39 h, quantitative; (ii) R^1NH_2, TBHP, CH_3OH, r.t., 48 h; (iii) EtI, K_2CO_3, CH_3CN, 60 °C, 3.5 days, quantitative; (iv) R^1NH_2, μω (Synthewave 402 reactor, Prolabo), 100−160 °C, 20−100 min.

Table 5. Effects of Leucettines L_{34-41} on the Catalytic Activity of Eight Purified Kinases[a]

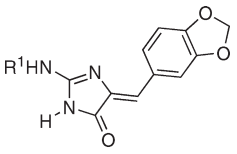

L_{34-41}

Compound	R^1	DYRK 1A	DYRK 2	CLK1	CLK3	GSK-3α/ß	CK1	CDK5/ p25	Pim1
$\mathbf{L_{31}}$	H	0.24	0.12	0.13	2.2	7.3	-	-	2.5
$\mathbf{L_{34}}$	CH_3CH_2	0.41	0.16	0.40	3.7	2.4	-	-	3.1
$\mathbf{L_{35}}$	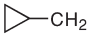	0.1	0.047	0.083	0.61	4.7	-	-	1.5
$\mathbf{L_{36}}$	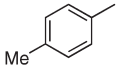	0.17	0.061	0.32	> 10	>10	-	-	9
$\mathbf{L_{37}}$	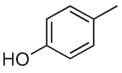	0.096	0.06	0.06	0.52	1.7	-	-	1.2
$\mathbf{L_{38}}$	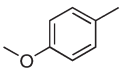	0.11	0.08	0.83	> 10	>10	-	-	> 10
$\mathbf{L_{39}}$	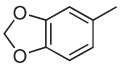	0.066	0.04	0.17	0.36	3	-	-	5
$\mathbf{L_{40}}$	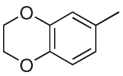	0.17	0.11	0.32	> 10	>10	-	-	> 10
$\mathbf{L_{41}}$	C_6H_5	0.040	0.035	0.015	4.5	0.41	> 10	-	4.1

[a] Compounds were tested at various concentrations on each kinase as described in Experimental Section. IC_{50} values are reported in μM. -, inactive at the highest concentration tested (10 μM); >10, inhibitory but IC_{50} >10 μM.

dx.doi.org/10.1021/jm200274d |J. Med. Chem. 2011, 54, 4172–4186

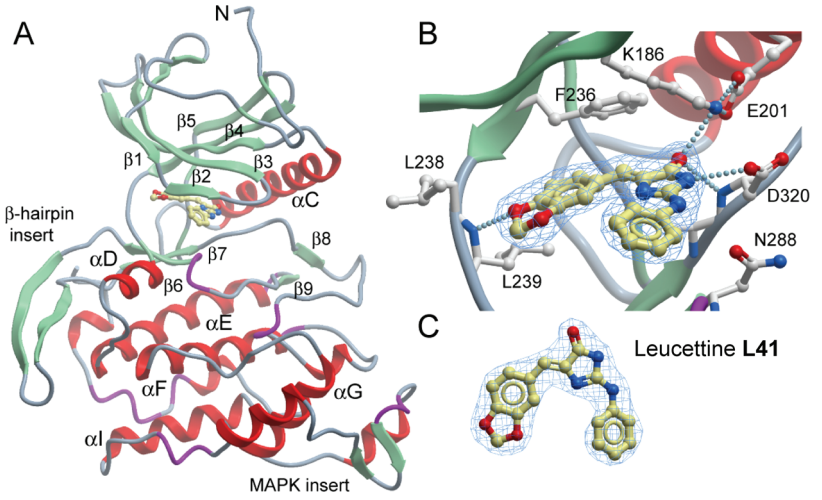

Figure 2. CLK3/leucettine $\mathbf{L_{41}}$ cocrystal structure. (A) Structure of CLK3 in ribbon diagram representation. Helices are shown in red, while β-sheets are shown in green. Leucettine $\mathbf{L_{41}}$ is shown in ball-and-stick representation. (B) Details of the interactions of leucettine $\mathbf{L_{41}}$ with the ATP binding pocket of CLK3 and selected side chains residues of CLK3 are shown in ball-and-stick representation. (C) $(2Fo - Fc)\alpha$-calc electron density for leucettine $\mathbf{L_{41}}$ calculated at the end of refinement using map coefficients output from REFMAC with resolution between 20 and 2.1 Å. The map is contoured at 2 σ.

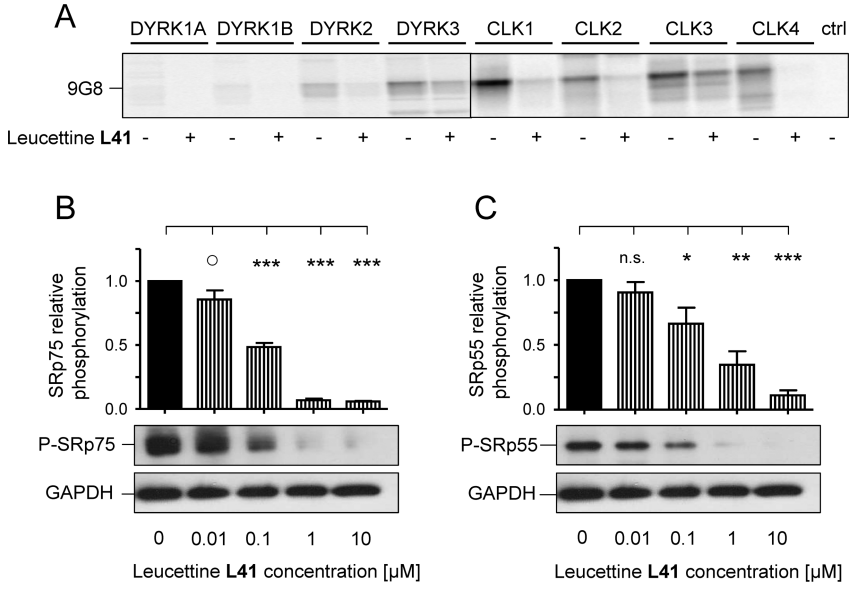

Figure 3. Leucettine inhibits the phosphorylation of SR proteins in vitro and in vivo. (A) Leucettine B $\mathbf{L_{41}}$ inhibits in vitro phosphorylation of the SR protein 6N98 by various DYRK and CLK kinases. Each individual kinase was incubated with 6N98 for 30 min in the presence or absence of 10 μM Leucettine $\mathbf{L_{41}}$. Phosphorylation of the substrate was analyzed by sodium dodecyl sulfate−polyacrylamide gel electrophoresis (SDS−PAGE) followed by autoradiography. (B,C) Leucettine inhibits the phosphorylation of SR proteins in endothelial cells. HMEC-1 cells were exposed to different concentrations of leucettine $\mathbf{L_{41}}$ and stimulated with 10 ng/mL TNF-α for 2 min. Phosphorylation of SRp75 (75 kDa) (B) and SRp55 (55 kDa) (C) was analyzed following SDS−PAGE by Western blotting using the phosphorylation-dependent antibody mAb1H4. GAPDH (36 kDa) was used as the loading control. Shown is the total band density as the mean ± SEM. The results are representative of at least 3 independent experiments. (○) $p < 0.15$, (*) $p < 0.01$, (**) $p < 0.001$, (***) $p < 0.0001$; n.s. indicates no significant difference.

favors the inhibition of DYRK1A and CLK1 in relation to GSK3α/β. For example, leucettine $\mathbf{L_{40}}$ showed a 100-fold higher affinity for DYRK1A versus GSK3α/β. Five compounds ($\mathbf{L_{36-37}}$ and $\mathbf{L_{39-41}}$) were identified as inhibitors of DYRK1A in the submicromolar range (IC_{50} = 40 to 90 nM), of which leucettine $\mathbf{L_{41}}$ was selected for further biological characterization. To the best of our knowledge, this new family of compounds represents one of the most potent inhibitors of DYRK1A.

Leucettine Inhibits Phosphorylation of Serine/Arginine-Rich Proteins in Vitro and in Vivo. The serine/arginine-rich (SR) proteins represent a family of highly conserved regulators of constitutive and alternative pre-mRNA splicing.[17,18] Phosphorylation of SR proteins by CLKs is known to regulate splicing events mediated by these proteins.[19]

We first investigated the effect of leucettine $\mathbf{L_{41}}$ on the in vitro phosphorylation of the SR protein 9G8 by DYRKS and CLKS.

dx.doi.org/10.1021/jm200274d |J. Med. Chem. 2011, 54, 4172–4186

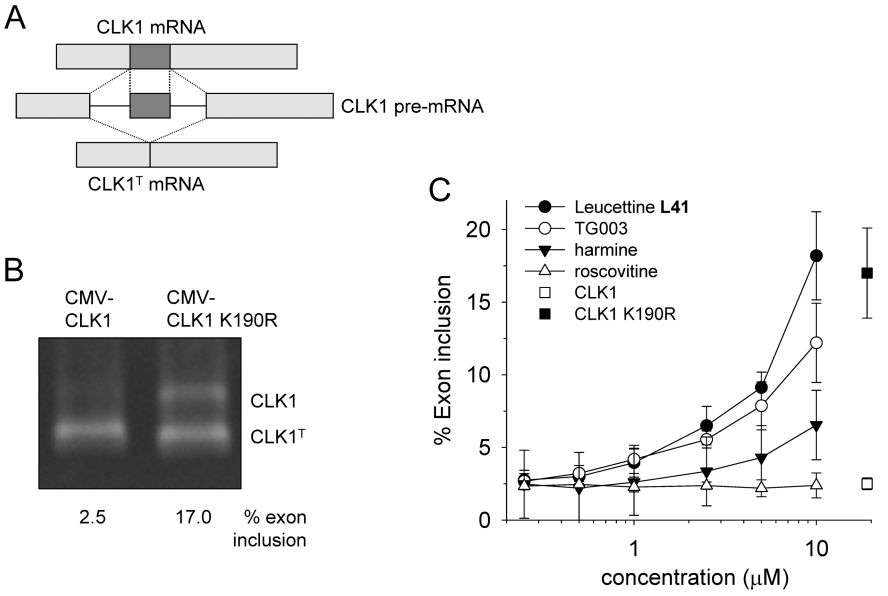

Figure 4. Leucettine alters alternative pre-mRNA splicing: CLK1 minigene reporter model. (A) Schematic representations of CLK1 minigene and its two alternative splicing products. The CLK1 minigene vector (CMV-CLK1) has three exons and two introns and produces two major alternatively spliced isoforms when expressed in cells. The predominant shorter form ($CLK1^T$) lacks the second exon of the minigene and does not produce an active kinase. Inclusion of the second exon produces mRNA for an active kinase (CLK1). The ratio of the two isoforms is regulated by the kinase activity of CLK1 itself and CLK4, resulting in an autoregulatory negative feedback of CLK1/CLK4 activity levels. (B) HeLa cells were transfected with CMV-CLK1 or its kinase inactive variant CMV-CLK1/K190R, which harbors the same minigene as CLK1 except for a missense mutation in its catalytic site. Three hours after transfection, the indicated doses of drugs were added to the cells. Cells were harvested 24 h after transfection, total RNA was extracted, and E1A splicing products were analyzed by RT-PCR. The spliced products were analyzed by RT-PCR and sequenced to confirm the specificity of PCR. The molar ratio of each isoform was analyzed by a 2100 Bioanalyzer (Agilent). (C) Effect of various kinase inhibitors on CLK1 minigene splicing. HeLa cells transfected with CMV-CLK1 were treated with varying doses of leucettine $\mathbf{L_{41}}$, TG003, harmine, or (*R*)-roscovitine. All cell cultures contained a final 0.5% concentration of DMSO. The exon inclusion ratios were calculated and plotted. Each plot represents the average of three independent samples. Error bars show the standard deviation.

Phosphorylation of 9G8 was recently shown to regulate alternative splicing of exon 10 of Tau.[14g] Recombinant 9G8 was incubated in the absence or presence of 10 μM leucettine $\mathbf{L_{41}}$ with DYRK1A, 1B, 2, 3, or CLK1, 2, 3, 4 (diluted to reach the same specific activity toward the RS peptide). Autoradiographic analysis of 9G8 phosphorylation showed that CLKs were more potent than DYRKs at phosphorylating this SR protein (Figure 3A). DYRK3 was the most efficient DYRK, while CLK1 was the most efficient CLK. Leucettine $\mathbf{L_{41}}$ was most potent at inhibiting 9G8 phosphorylation by DYRK2, DYRK3, CLK1, CLK2, and CLK4.

We next analyzed the effects of DYRKs/CLKs inhibition on the in vivo phosphorylation of two representative members of SR proteins. Human microvascular endothelial cells, HMEC-1 were treated with different concentrations of leucettine $\mathbf{L_{41}}$ and then stimulated with 10 ng/mL TNF-α (tumor necrosis factor-α) for 2 min. Proteins were then resolved by SDS−PAGE, and the phosphorylation of SR proteins was analyzed by Western blotting with phospho-specific anti-SR proteins antibodies. Results showed that leucettine $\mathbf{L_{41}}$ significantly reduced the phosphorylation of SRp75 and SRp55 in a concentration-dependent manner (Figure 3B,C). The phosphorylation state of both SR proteins was also reduced in cells that were not treated by TNF-α (data not shown). These results show that leucettine $\mathbf{L_{41}}$ is able to inhibit the phosphorylation of pre-mRNA splicing−controlling SR-rich proteins in a cellular context.

Leucettine Modulates Pre-mRNA Splicing. In order to confirm that leucettines are able to modulate alternative pre-mRNA splicing in a cellular context, we made use of a reporter cellular model.

This model was based on a synthetic CLK1 minigene and its alternative splicing products[20,21] (Figure 4). This minigene contained three exons and two introns and produces two major alternatively spliced isoforms when expressed in cells. The predominant shorter form ($CLK1^T$) lacks the second exon of the minigene and does not produce the active kinase. Inclusion of the second exon produces mRNA for active CLK1 (CLK1). The ratio of the two isoforms is regulated by the kinase activity of CLK1 itself and CLK4, resulting in an autoregulatory negative feedback of CLK1/CLK4 activity levels. HeLa cells were transfected with CMV-CLK1 or its kinase dead mutant CMV-CLK1-K190R. Three hours later, various kinase inhibitors were added to the cells: Leucettine $\mathbf{L_{41}}$, TG003 (a previously reported CLK inhibitor),[20] harmine (a DYRK/CLK inhibitor),[22] and roscovitine (a CDK inhibitor with slight inhibitory activity on DYRKs and no activity on CLKs).[23] Twenty-four hours after transfection, cells were harvested, total RNA was extracted, and splicing products were analyzed by RT-PCR. The molar ratio of each isoform was analyzed by a 2100 Bioanalyzer (Agilent). Both leucettine $\mathbf{L_{41}}$ and TG003, and harmine to a lesser extent, but not roscovitine, increased the exon inclusion ratio in a dose-dependent manner, reaching a level similar to that seen with the kinase dead CLK1 (Figure 4). This result highly suggests that Leucettine $\mathbf{L_{41}}$ (even better than TG003) is able to modulate alternative splicing by the inhibition of CLKs.

CONCLUSIONS

Data presented in this study demonstrate the promising kinase inhibitory potential of derivatives and analogues of the natural product leucettamine B, a 2-aminoimidazolone produced by marine sponges. Critical for affinity enhancement is the introduction of a phenyl ring at position R^1. Affinity improvements are possibly a consequence of the limited flexibility of the phenyl ring (compared to that of alkyl or benzyl groups), that permits more extensive stabilizing hydrophobic interactions with residues of the gly loop. Additionally, an affinity gain in analogues $\mathbf{L_{31}}$ and $\mathbf{L_{34-41}}$ results from the increased hydrogen bonding potential of the secondary amine NH adjacent to the phenyl ring, as an outcome result of the orbital delocalization of the hydrogen over the aromatic ring. At the same time, there is a possibility for developing highly selective dual DYRK1A and CLK inhibitors based on the 2-aminoimidazolone scaffold. Although a clear relationship between the different substitution schemes of positions R^1 and R^2 and selectivity was not apparent, certain combinations afford compounds that interacted with DYRK1A or CLK with an up to 100-fold improved affinity compared to that of GSK-3α/β (e.g., $\mathbf{L_{40}}$). Small differences in the residues comprising the binding pocket of each kinase do exist, and this could result in the deviations observed in the binding mode established by the CLK3-$\mathbf{L_{41}}$ co-crystal structure. Docking experiments show that a reversed binding mode is possible in the DYRK1A ATP-binding cavity. In this mode, the interaction between the lactam C═O and NH of leucettamines $\mathbf{L_{31}}$ and $\mathbf{L_{34-41}}$ and the kinase hinge would explain the pronounced affinity improvement of these analogues toward DYRK1A and CLK1 compared to that of GSK-3α/β.

Alternative pre-mRNA splicing is a fundamental mechanism for posttranscriptional regulation of gene expression.[24] CLKs modulate the phosphorylation state of SR proteins, which in turn regulates the localization, substrate affinity and splicing activity of SR proteins in alternative splicing processes.[17,19,25] The pharmacological inhibition of CLKs was demonstrated to affect the alternative splicing of important vascular proteins, such as tissue factor or vascular endothelial growth factor.[19,26] Here, we show that leucettine $\mathbf{L_{41}}$ reduces the CLK-mediated phosphorylation of SRp75 and SRp55 under normal as well as pro-inflammatory conditions in a concentration-dependent manner. Therefore, leucettines are adequate molecular biological tools for examining the role of CLKs in the control of alternative splicing processes via regulating the phosphorylation of SR proteins. Modulation of alternative splicing by low molecular weight kinase inhibitors will be of great interest in the fundamental study of this key physiological regulatory mechanism and its regulation by CLKs and DYRKs. Pharmacological inhibitors like leucettines may also prove to be of key importance in the design of therapeutically active regulators of alternative pre-mRNA splicing when abnormally balanced in human disease. For example, CLK and DYRK inhibitors such as leucettines may find important applications in Alzheimer's disease and Down syndrome indications. There is indeed growing evidence for important links between the activity of these kinases and these diseases:[14,15] (1) DYRK1A phosphorylates key players in AD, namely, APP,[14d] Tau,[14c] presenilin,[14c] and septin-4,[14f] (2) DYRK1A acts as a priming kinase,[14a] allowing its substrates to be further phosphorylated by GSK-3, a key kinase in AD,[39] (3) the DYRK1A gene is located on chromosome 21, and its overexpression in DS is associated with early AD phenotype observed in DS patients,[15] (4) genetic studies in humans demonstrate a strong link between the DYRK1A gene and amyloid-β production,[14b] (5) DYRK1A is involved in alternate splicing of Tau pre-mRNA (the balance between Tau 3R/4R splicing variants is altered in AD),[14g−i,15c,j] and (6) CLKs and DYRKs are key regulators of pre-mRNA splicing and therefore also control the level of Tau 3R/4R variants. Altogether, these data make DYRKs and CLKs very attractive therapeutic targets for AD.

EXPERIMENTAL SECTION

Chemistry. *General Methods.* Reagents obtained from commercial suppliers were used without further purification. Acetonitrile was distilled over calcium chloride after standing overnight and stored over 3 Å molecular sieves. Thin-layer chromatography (TLC) was accomplished on 0.2-mm precoated plates of silica gel 60 F-254 (Merck), and visualization was made with ultraviolet light (254 and 312 nm) or with a fluorescence indicator. Melting points were determined on a Kofler melting point apparatus and were uncorrected. ^{1}H NMR spectra were recorded on Bruker AC 300 P (300 MHz) and Bruker ARX 200 (200 MHz) spectrometers, and ^{13}C NMR spectra on a Bruker AC 300 P (75 MHz) spectrometer. Chemical shifts are expressed in parts per million downfield from tetramethylsilane (TMS) as an internal standard. Proton coupling constants (J values) are expressed in hertz using the following designations: s (singlet), d (doublet), br s (broad singlet), q (quartet), and m (multiplet). Reactions under microwave irradiations were realized in a Synthewave 402 apparatus (Merck Eurolab, Div. Prolabo, France). The microwave instrument consists of a continuous focused microwave power output from 0 to 300W. All of the experiments were performed using stirring option. The target temperature was reached with a ramp of 3 min, and the chosen microwave power stayed constant to hold the mixture at this temperature. The reaction temperature is monitored using a calibrated infrared sensor, and the reaction time includes the ramp period. The mass spectra (HRMS) were taken on a Varian Mat 311 at an ionizing potential of 70 eV in the Centre Régional de Mesures Physiques de l'Ouest (CRMPO, Rennes). All tested compounds $\mathbf{L_x}$ possessed a purity of ≥95% as verified by elemental analyses by comparison with the theoretical values.

*General Procedure for the Synthesis of Leucettamine B Derivatives from (5Z)-5-[(1,3-Benzodioxol-5-yl)methylene]-3-methyl-2-thioxo-imidazolin-4-one (**3a**).* To a solution of (5Z)-5-[(1,3-benzodioxol-5-yl)methylene]-3-methyl-2-thioxo-imidazolin-4-one (**3a**) (200 mg, 0.76 mmol) in methanol (20 mL) and commercial amine (15.2 mmol) in a 10 mL round-bottomed flask, provided with a magnetic stirrer and reflux condenser, was added a solution of TBHP (70%, 0.32 mL, 2.3 mmol) in one portion. The solution was stirred for 48 h at room temperature. The solvent was evaporated under reduced pressure with a rotary evaporator, and the crude residue was submitted to purification by chromatography on silica gel using dichloromethane−methanol as eluent.

(5Z)-5-[(1,3-Benzodioxol-5-yl)methylene]-3-methyl-2-methylamino-3,5-dihydro-4*H*-imidazol-4-one ($\mathbf{L_1}$): The title compound was prepared from methylamine (40%) (dichloromethane−methanol, 98/2, R_f = 0.18). Yellow powder, yield = 40%. Mp = 224−226 °C. ^{1}H NMR (300 MHz, DMSO-d_6): δ = 2.96 (d, 3H, J = 4.4 Hz, CH_3), 3.03 (s, 3H, CH_3), 6.03 (s, 2H, OCH_2O), 6.34 (s, 1H, =CH), 6.92 (d, 1H, J = 8.1 Hz, Ar), 7.43 (d, 1H, J = 8.1 Hz, Ar), 7.62 (br q, 1H, J = 4.4 Hz, NH), 7.98 (s, 1H, Ar). ^{13}C NMR (75 MHz, DMSO-d_6): δ = 25.9, 28.3, 101.5, 108.7, 109.6, 111.9, 125.7, 131.2, 139.4, 147.1, 148.4, 159.5, 169.4. Anal. Calcd for $C_{13}H_{13}N_3O_3$: C, 60.23; H, 5.05; N, 16.21. Found: C, 60.17; H, 4.99; N, 16.24.

*Synthesis of Leucettamine B Derivatives from (5Z)-5-[(1,3-Benzodioxol-5-yl)methylene]-3-methyl-2-ethylthio-3,5-dihydro-4H-imidazol-4-one (**4a**). Method A (Thermic Process).* In a 10 mL round-bottomed flask, provided with a magnetic stirrer and reflux condenser, a solution of (5Z)-5-[(1,3-benzodioxol-5-yl)methylene]-3-methyl-2-ethylthio-3,5-dihydro-4*H*-imidazol-4-one (**4a**) (300 mg, 1 mmol) and the corresponding primary

dx.doi.org/10.1021/jm200274d | J. Med. Chem. 2011, 54, 4172–4186

amine (10 mmol) was heated at reflux during 3 days. After cooling down to room temperature, the excess of primary amine was evaporated under reduced pressure with a rotary evaporator, and the crude residue was submitted to purification by chromatography on silica gel with the appropriate eluent or was precipitated with Et_2O or EtOH.

*(5Z)-5-[(1,3-Benzodioxol-5-yl)methylene]-3-methyl-2-propylamino-3,5-dihydro-4H-imidazol-4-one (**L3**).* The title compound was prepared from propylamine using method A in 47% yield as a yellow powder; mp = 190−192 °C. ^{1}H NMR (300 MHz, $CDCl_3$): δ = 1.02 (t, 3H, J = 7.4 Hz, CH_3), 1.72−1.75 (m, 2H, CH_2), 3.11 (s, 3H, CH_3), 3.54 (t, 2H, J = 6.2 Hz, CH_2), 4.95 (br s, 1H, NH), 5.98 (s, 2H, OCH_2O), 6.62 (s, 1H, =CH), 6.81 (d, 1H, J = 8.1 Hz, Ar), 7.34 (dd, 1H, J = 8.1, 1.2 Hz, Ar), 7.99 (d, 1H, J = 1.2 Hz, Ar). ^{13}C NMR (75 MHz, $CDCl_3$): δ = 11.5, 22.8, 25.2, 43.7, 101.1, 108.4, 110.3, 116.8, 126.1, 130.2, 138.1, 147.6, 147.7, 157.2, 170.4. HRMS, m/z = 287.1279 found (calculated for $C_{15}H_{17}N_3O_3$, $M^{+\bullet}$ requires 287.1270). Anal. Calcd for $C_{15}H_{17}N_3O_3$: C, 62.71; H, 5.96; N, 14.62. Found: C, 62.69; H, 5.98; N, 14.64.

Method B (Microwave Irradiation Process). A mixture of (5Z)-5-[(1,3-benzodioxol-5-yl)methylene]-3-methyl-2-ethylthio-3,5-dihydro-4*H*-imidazol-4-one (**4a**) (300 mg, 1 mmol) and primary amine (5 mmol) was placed in a cylindrical quartz reactor (Ø = 1.8 cm). The reactor was then introduced into a Synthewave 402 Prolabo microwave reactor (P = 300 W). The stirred mixture was irradiated at the appropriate reaction temperature (with a power level ranging from 50 to 100%) for an appropriate reaction time (20−100 min.). After microwave dielectric heating, the crude reaction mixture was allowed to cool down at room temperature, and ethanol, diethyl ether, or chloroform (10 mL) was added directly into the cylindrical quartz reactor. The resulting precipitated product was filtered off and was purified by recrystallization from ethanol, diethyl ether, or chloroform.

*(5Z)-5-[(1,3-Benzodioxol-5-yl)methylene]-3-methyl-2-(2-hydroxyethyl)amino-3,5-dihydro-4H-imidazol-4-one (**L11**).* The title compound was prepared from 4 equivalents of 2-hydroxyethylamine using method B (reaction time = 50 min, temperature = 120 °C) in 33% yield as a yellow powder; mp = 180−182 °C. ^{1}H NMR (300 MHz, DMSO-d_6): δ = 3.05 (s, 3H, CH_3), 3.44−3.49 (m, 2H, CH_2), 3.61−3.65 (m, 2H, CH_2), 4.84−4.88 (br s, 1H, OH), 6.02 (s, 2H, OCH_2O), 6.36 (s, 1H, =CH), 6.90 (d, 1H, J = 7.0 Hz, Ar), 7.34 (d, 1H, J = 7.0 Hz, Ar), 7.66 (s, 1H, Ar), 7.91−7.97 (br s, 1H, NH). ^{13}C NMR (75 MHz, DMSO-d_6): δ = 25.5, 43.9, 59.3, 100.9, 108.2, 109.4, 112.7, 125.1, 130.3, 138.7, 146.6, 147.1, 158.2, 169.5. HRMS, m/z = 289.1055 found (calculated for $C_{14}H_{15}N_3O_4$, $M^{+\bullet}$ requires 289.1063). Anal. Calcd for $C_{14}H_{15}N_3O_4$: C, 58.13; H, 5.23; N, 14.53. Found: C, 58.19; H, 5.20; N, 14.55.

Biochemistry. *Buffers. Buffer A.* 10 mM $MgCl_2$, 1 mM EGTA, 1 mM DTT, 25 mM Tris-HCl at pH 7.5, and 50 μg heparin/mL.

Buffer C. 60 mM *ss*-glycerophosphate, 30 mM *p*-nitrophenylphosphate, 25 mM Mops (pH 7.2), 5 mM EGTA, 15 mM $MgCl_2$, 1 mM DTT, 0.1 mM sodium vanadate, and 1 mM phenylphosphate.

Kinase Preparations and Assays. Kinase activities were assayed in buffer A or C, at 30 °C, at a final ATP concentration of 15 μM. Blank values were subtracted and activities expressed in percent of the maximal activity, i.e., in the absence of inhibitors. Controls were performed with appropriate dilutions of DMSO. The kinase peptide substrates were obtained from Proteogenix (Oberhausbergen, France).

DYRK1A and *DYRK2* (respectively rat and human, recombinant, expressed in *E. coli* as a GST fusion protein) were purified by affinity chromatography on glutathione-agarose and assayed in buffer A (+ 0.15 mg BSA/mL) using Woodtide (KKISGRLSPIMTEQ) (1.5 μg/assay) as a substrate, in the presence of 15 μM [γ-^{33}P] ATP (3,000 Ci/mmol; 10 mCi/mL) in a final volume of 30 μL. After 30 min, incubation at 30 °C, the reaction was stopped by harvesting onto P81 phosphocellulose papers (Whatman) using a FilterMate harvester (Packard) and were washed in 1% phosphoric acid. Scintillation fluid was added and the radioactivity measured in a Packard counter.

CLK1 and *CLK3* (mouse, recombinant, and expressed in *E. coli* as GST fusion proteins) were assayed in buffer A (+ 0.15 mg BSA/mL) with RS peptide (GRSRSRSRSRSR) (1 μg/assay).

CDK5/p25 (human, recombinant) was prepared as previously described.[27] Its kinase activity was assayed in buffer C, with 1 mg histone H1/mL.

GSK-3α/β (porcine brain, native) was assayed in buffer A and using a GSK-3 specific substrate (GS-1: YRRAAVPPSPSLSRHSSPHQSpED-EEE) (pS stands for phosphorylated serine).[28]

CK1δ/ε (porcine brain, native) was assayed in 3-fold diluted buffer C, using 25 μM CKS peptide (RRKHAAIGpSAYSITA), a CK1-specific substrate.[29]

Pim1 (human recombinant) was assayed in buffer C, with 1 mg histone H1/mL.

CLK3/Inhibitor Cocrystallization and Structure Determination

Cloning, Protein Expression, and Purification. An expression construct of CLK3A was made by subcloning a PCR fragment encoding R134 to L475 into the pLIC-SGC vector using ligation independent cloning. The expressed protein included an N-terminal hexahistidine tag and a TEV (tobacco etch virus) protease tag cleavage site. The cloned vector was freshly transformed in competent *E. coli* BL21(DE3)-R3-pRARE2 cells (phage-resistant derivative of BL21(DE3)), with a pRARE plasmid, which were grown overnight at 37 °C in 5 mL of Luria−Bertani medium (LB-broth) containing 50 μg/mL kanamycin and 34 μg/mL chloramphenicol. This culture was diluted 1:1000 in fresh medium and cell growth was allowed at 37 °C to an optical density of about 0.5 (OD600) before the temperature was decreased to 18 °C. Protein expression was induced overnight at 18 °C with 0.1 mM isopropyl-β-D-thiogalactopyranoside (IPTG). The bacteria were harvested by centrifugation and were frozen at −20 °C. Cells were resuspended in lysis buffer (50 mM HEPES, pH 7.5 at 25 °C, 500 mM NaCl, 5 mM imidazole, 5% glycerol, 0.5 mM TCEP, and 50 mM L-Arg and L-Glu) in the presence of protease inhibitor cocktail (1 μL/mL) and lysed using an EmulsiFlex-C5 high pressure homogenizer at 4 °C. DNA was separated from protein using DEAE cellulose (DE52, Whatman). Ten grams of resin was suspended in a 2.5 × 20 cm column. The resin was hydrated in 2.5 M NaCl, then washed with 20 mL of binding buffer (50 mM HEPES, 500 mM NaCl, 5% glycerol, and 50 mM L-Arg and L-Glu) prior to loading the sample. The column flow-through was collected and was applied to a nickel-nitrilotriacetic acid agarose column (Ni-NTA, Qiagen Ltd.)., 5 mL, equilibrated in lysis buffer). The column was washed with 30 mL of lysis buffer. The protein was eluted using a step elution of imidazole in lysis buffer (50, 100, 150, 2 × 250 mM imidazole in 50 mM HEPES, pH 7.5 at 25 °C, 500 mM NaCl, 50 mM L-Arg and L-Glu). All fractions were collected and monitored by SDS−PAGE. After the addition of 10 mM dithiothreitol (DTT), the eluted protein was treated overnight at 4 °C with TEV protease. The protein was further purified with size exclusion chromatography on a Superdex 75 16/60 HiLoad gel filtration column on an ÄktaPrime plus system (GE/Amersham Biosciences). Samples were monitored by SDS−PAGE and concentrated to 11 mg/mL in the elution buffer, 10 mM Hepes, pH 7.5, 500 mM NaCl, and 50 mM L-Arg and L-Glu and were used for crystallization.

Crystallization. Aliquots of the purified proteins were set up for crystallization using the vapor diffusion method. Coarse screens were typically setup onto Greiner or SWISSCI 3-well plates using three different drop ratios of precipitant to protein per condition. Initial hits were optimized further, and suitable crystals were obtained at a protein concentration of 11 mg/mL and a buffer containing 0.1 M Bis-Tris propane at pH 7.5, 20.0% polyethylene glycol (PEG) 3350, and 10.0% ethylene glycol. Crystals grew to diffracting quality within 1−3 weeks.

Table 6. CLK3/Leucettine L_{41} Co-Crystal Structure[a]

Data Collection	
PDB ID	3raw
space group	$P2_1$
cell dimensions:	
a, b, c (Å)	61.67, 122.42, 69.28
α, β, γ (deg)	90.0, 92.6, 90.0
resolution[b] (Å)	2.09 (2.09−2.2)
unique observations[b]	59553 (8602)
completeness[b] (%)	98.02 (97.1)
redundancy[b]	3.9 (3.9)
R_{merge}[b]	0.09 (0.755)
$I/\sigma I$[b]	8.4 (2.0)
Refinement	
resolution (Å)	2.09
R_{work}/R_{free} (%)	18.2/22.1
number of atoms (protein/other/water)	5928/72/247
B-factors (Å^2) (protein/ligand/water)	22.3/32.5/25.0
rmsd bonds (Å)	0.016
rmsd angles (deg)	1.520
Ramachadran:	
favored (%)	99.3
allowed (%)	0.3
disallowed (%)	0

[a] Statistics of the data set used and of the refined structures. [b] Values in parentheses correspond to the highest resolution shell.

Data Collection and Structure Solution. Crystals were cryo-protected using the well solution supplemented with 20% additional ethylene glycol and were flash frozen in liquid nitrogen. Data were collected to a resolution of 2.09 Å at the SLS (Swiss Light Source) beamline SA X10. Indexing integration and scaling was carried out using MOSFLM[30] and SCALA[31] (I, III) or HKL2000[32] (II). Initial phases were calculated by molecular replacement with PHASER[33] using the structure of CLK1 that has been determined earlier in our laboratory.[34] Initial models were built by ARP/wARP,[35] and building was completed manually with COOT.[36] Refinement was carried out in REFMAC5.[37] Data collection and refinement statistics can be found in Table 6.

In Vitro SR Protein Phosphorylation. In vitro phosphorylation of the 9G8 SR protein was carried out in the absence or presence of 10 μM leucettine $\mathbf{L_{41}}$. The phosphorylation reactions were carried out at 30 °C for 30 min using 15 μM [γ-^{33}P] ATP (3000 Ci/mmol, 10 mCi/mL) in the presence of the different DYRKs and CLKs diluted to provide the same specific activity using the RS peptide as a substrate (0.35 μL DYRK1A, 0.08 μL DYRK1B, 0.08 μL DYRK2, 2 μL DYRK3, 0.8 μL CLK1, 0.16 μL CLK2, 0.48 μL CLK3, and 0.26 μL CLK4). The incubation buffer contained 2 mM $MgCl_2$, 0.2 mM EGTA, 1.7 mM DTT, 5 mM Tris-HCl, pH 7.5, 10 μg heparin/mL, 3 μg BSA, 0.1% DMSO, and 87 ng of recombinant SR protein 9G8 in the presence or absence of 10 μM Made 44. The reactions were stopped by adding loading buffer followed by heat denaturation, and the proteins were resolved on a SDS−PAGE gel. Phosphorylation of the substrate was assessed by autoradiography.

In Vivo SR Protein Phosphorylation. *Cell Culture.* Human microvascular endothelial cells (HMEC-1) were cultured in endothelial cell medium (PAA Laboratories GmbH, Pasching, Austria) containing 5% fetal calf serum (FCS) at 37 °C in a humidified incubator (5% CO_2, 95% air). Cells from passages 2 to 8 were used. For inhibition experiments, HMEC-1 were switched to endothelial cell basal medium (without FCS) for 1 h and then pretreated with different concentration of leucettine $\mathbf{L_{41}}$ for 1 h. After that, cells were stimulated or not with 10 ng/mL TNF-α (Sigma Aldrich, St Louis, USA). The phosphorylation state of SR proteins was characterized 2 min post-induction of the cells by Western blot analyses. Positive controls were stimulated only with TNF-α, and negative controls were nontreated.

Western Blotting. Whole cell lysates of inhibited, stimulated, and nontreated HMEC-1 cells were subjected to Western blot analysis as previously described.[38] The change in protein amount was quantified by densitometry. For the detection of phosphorylated SR proteins, monoclonal antibody mAb1H4 (Invitrogen GmbH, Karlsruhe, Germany) was used.

Statistical Analysis. All data were expressed as the mean ± SEM. Data were analyzed by Student's *t*-test or one-way ANOVA. A probability value ≤0.05 was deemed significant.

Alternative Pre-mRNA Splicing and CLK Inhibition in Cells. *CLK1 Minigene and Its Alternative Splicing Products.* All experiments were carried out as described in previous papers with minor modifications.[20,21]

■ ASSOCIATED CONTENT

Supporting Information. General experimental methods and characterization data (^{1}H and ^{13}C NMR, HRMS, and elemental analysis) for all compounds. This material is available free of charge via the Internet at http://pubs.acs.org.

Accession Codes

The models and structure factors have been deposited with PDB accession codes 3raw.

■ AUTHOR INFORMATION

Corresponding Author

*(L.M. (biology)) Tel: +33.(0)2.98.29.23.39. Fax: +33.5(0)2.98.29.25.26 E-mail: meijer@sb-roscoff.fr. (F.C. (chemistry)) E-mail: francois.carreaux@univ-rennes1.fr. Tel: +33.(0)2.23.23.57.34. Fax: 33.(0)2.99.28.69.55 (J.P.B. (chemistry)) Tel: +33.(0)2.23.23.66.03. Fax: 33.(0)2.23.23.63.74. E-mail: jean-pierre.bazureau@univ-rennes1.fr.

■ ACKNOWLEDGMENT

We thank Dr. Pascal Loyer, INSERM, Rennes, for providing the 9G8 protein. We are grateful to the "Conseil Régional de Bretagne: Programme 1042" for a research fellowship (contract number 20046919 to S.R.). The financial support for this program carried out under the "Cancéropôle Grand Ouest/Institut National du Cancer", contracts PRIR 04-8390 and ACI 04-2254, are gratefully acknowledged. We also thank Merck Eurolab Prolabo (Fr.) for providing the Synthewave 402 apparatus. L.M.'s funding for this project included "CRITT Santé Bretagne", "Fondation Jérôme Lejeune", "Association France-Alzheimer (Finistère)", and the FUI PharmaSea project. S.K. is an investigator of the Structural Genomics Consortium (SGC), a registered charity (no. 1097737) funded by the Wellcome Trust, GlaxoSmithKline, Genome Canada, the Canadian Institutes of Health Research, the Ontario Innovation Trust, the Ontario Research and Development Challenge Fund, the Canadian Foundation for Innovation, VINNOVA, The Knut and Alice Wallenberg Foundation, The Swedish Foundation for Strategic Research, and Karolinska Institutet.

■ ABBREVIATIONS

BSA, bovine serum albumin; CDKs, cyclin-dependent kinases; CK1, casein kinase 1; CLKs, cdc2-like kinases; DMSO, dimethylsulfoxide; DTT, dithiothreitol; DYRKs, dual-specificity, tyrosine phosphorylation regulated kinases; FCS, fetal calf serum; gHSQMBC, gradient heteronuclear single quantum multiple bond correlation; GSH, glutathione; GSK-3, glycogen synthase kinase-3; GST, glutathione-*S*-transferase; HMEC, human microvascular endothelial cells; MEK-1, mitogen-activated protein kinase 1; PBS, phosphate-buffered saline; SRp, serine/arginine-rich proteins; TNF-α, tumor necrosis factor α

■ REFERENCES

(1) (a) Kornprobst, J.-M. *Encyclopedia of Marine Natural Products*; Wiley: New York, 2010; Vol. 3, pp 1680. (b) Morris, J. C.; Phillips, A. J. Marine natural products: synthetic aspects. *Nat. Prod. Rep.* **2010**, *27*, 1186–1203. (c) Thomas, T. R.; Kavlekar, D. P.; LokaBharathi, P. A. Marine drugs from sponge-microbe association: a review. *Mar. Drugs* **2010**, *8*, 1417–1468.

(2) (a) Blunt, J. W.; Copp, B. R.; Munro, M. H.; Northcote, P. T.; Prinsep, M. R. Marine natural products. *Nat. Prod. Rep.* **2010**, *27*, 165–237. (b) Glaser, K. B.; Mayer, A. M. A renaissance in marine pharmacology: From preclinical curiosity to clinical reality. *Biochem. Pharmacol.* **2009**, *78*, 440–448. (c) Molinski, T. F.; Dalisay, D. S.; Lievens, S. L.; Saludes, J. P. Drug development from marine natural products. *Nat. Rev. Drug Discovery* **2009**, *8*, 69–85. (d) Waters, A. L.; Hill, R. T.; Place, A. R.; Hamann, M. T. The expanding role of marine microbes in pharmaceutical development. *Curr. Opin. Biotechnol.* **2010**, *21*, 780–786. (e) Mayer, A. M.; Rodríguez, A. D.; Berlinck, R. G.; Fusetani, N. Marine pharmacology in 2007−8: Marine compounds with antibacterial, anticoagulant, antifungal, anti-inflammatory, antimalarial, antiprotozoal, antituberculosis, and antiviral activities; affecting the immune and nervous systems, and other miscellaneous mechanisms of action. *Comp. Biochem. Physiol., Part C: Toxicol. Pharmacol.* **2011**, *153*, 191–222. (f) Villa, F. A.; Gerwick, L. Marine natural product drug discovery: Leads for treatment of inflammation, cancer, infections, and neurological disorders. *Immunopharmacol. Immunotoxicol.* **2010**, *32*, 228–237. (g) Mayer, A. M.; Glaser, K. B.; Cuevas, C.; Jacobs, R. S.; Kem, W.; Little, R. D.; McIntosh, J. M.; Newman, D. J.; Potts, B. C.; Shuster, D. E. The odyssey of marine pharmaceuticals: a current pipeline perspective. *Trends Pharmacol. Sci.* **2010**, *31*, 255–265. (h) Yasuhara-Bell, J.; Lu, Y. Marine compounds and their antiviral activities. *Antiviral Res.* **2010**, *86*, 231–240.

(3) Chan, G. W.; Mong, S.; Hemling, M. E.; Freyer, A. J.; Offen, P. M.; De Brosse, C. W.; Sarau, H. M.; Westley, J. W. New leukotriene B4 receptor antagonist: leucettamine A and related imidazole alkaloids from the marine sponge *Leucetta microraphis*. *J. Nat. Prod.* **1993**, *56*, 116–121.

(4) Watanabe, K.; Tsuda, Y.; Iwashima, M.; Iguchi, K. A new bioactive triene aldehyde from the marine sponge *Leucetta microraphis*. *J. Nat. Prod.* **2000**, *63*, 258–260.

(5) (a) Davis, R. A.; Aalbersberg, W.; Meo, S.; Moreira da Rocha, R.; Ireland, C. M. The isolation and synthesis of polyandrocarpamines A and B. Two new 2-aminoimidazolone compounds from the Fijian ascidian, *Polyandrocarpa sp*. *Tetrahedron Lett.* **2002**, *58*, 3263–3269. (b) Davis, R. A.; Baron, P. S.; Neve, J. E.; Cullinane, C. A microwave-assisted stereoselective synthesis of polyandrocarpamines A and B. *Tetrahedron Lett.* **2008**, *50*, 880–882.

(6) (a) Lindel, T.; Hoffmann, H. Synthesis of dispacamide from the marine sponge *Agelas dispar*. *Tetrahedron Lett.* **1997**, *38*, 8935–8938. (b) Fresneda, P. M.; Molina, P.; Sanz, M. A. A convergent approach to midpacamide and dispacamide pyrrole-imidazole marine alkaloids. *Tetrahedron Lett.* **2001**, *42*, 851–854. (c) Travert, N.; Al-Mourabit, A. A likely biogenetic gateway linking 2-aminoimidazolinone metabolites of sponges to proline: spontaneous oxidative conversion of the pyrrole-proline-guanidine pseudo-peptide to dispacamide A. *J. Am. Chem. Soc.* **2004**, *126*, 10252–10253. Erratum in: *J. Am. Chem. Soc.* **2005**, *127*, 10454.

(7) (a) Hollenbeak, K. H.; Schmitz, F. J. Aplysinopsin: antineoplastic tryptophan derivative from the marine sponge *Verongia spengelii*. *Lloydia* **1977**, *40*, 479–481. (b) Singh, S. N.; Bhatnagar, S.; Fatma, N.; Chauhan, P. M.; Chatterjee, R. K. Antifilarial activity of a synthetic marine alkaloid, aplysinopsin (CDRI Compound 92/138). *Trop. Med. Int. Health* **1997**, *2*, 535–543.

(8) (a) Cimino, G.; de Rosa, S.; de Stefano, S.; Mazzarella, L.; Puliti, R.; Sodano, G. Isolation & X-ray crystal structure of a novel bromo-compound from two marine sponges. *Tetrahedron Lett.* **1982**, *23*, 767–768. (b) Sharma, G. M.; Buyer, J.; Pomerantz, M. W. Characterization of a yellow compound isolated from the marine sponge *Phakellia flabellata*. *J. Chem. Soc. Chem. Commun.* **1980**, *10*, 435–436. (c) Williams, D. H.; Faulkner, J. Isomers and tautomers of hymenialdisine and debromohymenialdisine. *Nat. Prod. Lett.* **1996**, *9*, 57–64. (d) Xu, Y. Y.; Yakushijin, K.; Horne, D. A. Synthesis of C(11)N(5) Marine sponge alkaloids: (±)-hymenin, stevensine, hymenialdisine, and debromohymenialdisine. *J. Org. Chem.* **1997**, *62*, 456–464. (e) Papeo, G.; Posteri, H.; Borghi, D.; Varasi, M. A new glycociamidine ring precursor: syntheses of (Z)-hymenialdisine, (Z)-2-debromohymenialdisine, and (±)-endo-2-debromohymenialdisine. *Org. Lett.* **2005**, *7*, 5641–5644. (f) Nguyen, T. N.; Tepe, J. J. Preparation of hymenialdisine, analogues and their evaluation as kinase inhibitors. *Curr. Med. Chem.* **2009**, *16*, 3122–3143.

(9) (a) Meijer, L.; Thunnissen, A. M. W. H.; White, A.; Garnier, M.; Nikolic, M.; Tsai, L. H.; Walter, J.; Cleverley, K. E.; Salinas, P. C.; Wu, Y. Z.; Biernat, J.; Mandelkow, E. M.; Kim, S.-H.; Pettit, G. R. Inhibition of cyclin-dependent kinases, GSK-3β and casein kinase 1 by hymenialdisine, a marine sponge constituent. *Chem. Biol.* **2000**, *7*, 51–63. (b) Wan, Y.; Hur, W.; Cho, C. Y.; Liu, Y.; Adrian, F. J.; Lozach, O.; Bach, S.; Mayer, T.; Fabbro, D.; Meijer, L.; Gray, N. S. Synthesis and target identification of hymenialdisine analogs. *Chem. Biol.* **2004**, *11*, 247–259.

(10) Tasdemir, D.; Mallon, R.; Greenstein, M.; Feldberg, L. R.; Kim, S. C.; Collins, K.; Wojciechowicz, D.; Mangalindan, G. C.; Concepción, G. P.; Harper, M. K.; Ireland, C. M. Aldisine alkaloids from the Philippine sponge *Stylissa massa* are potent inhibitors of mitogen-activated protein kinase kinase-1 (MEK-1). *J. Med. Chem.* **2002**, *45*, 529–532.

(11) (a) Sharma, V.; Tepe, J. J. Potent inhibition of checkpoint kinase activity by a hymenialdisine-derived indoloazepine. *Bioorg. Med. Chem. Lett.* **2004**, *14*, 4319–4321. (b) Parmentier, J. G.; Portevin, B.; Golsteyn, R. M.; Pierré, A.; Hickman, J.; Gloanec, P.; De Nanteuil, G. Synthesis and CHK1 inhibitory potency of Hymenialdisine analogues. *Bioorg. Med. Chem. Lett.* **2009**, *19*, 841–844.

(12) (a) Molina, P.; Almendros, P.; Fresneda, P. M. An iminophosphorane-mediated efficient synthesis of the alkaloid leucettamine B of marine of origin. *Tetrahedron Lett.* **1994**, *35*, 2235–2236. (b) Roué, N.; Bergman, J. Synthesis of the marine alkaloid leucettamine B. *Tetrahedron* **1999**, *55*, 14729–14738. (c) Chérouvrier, J. R.; Boissel, J.; Carreaux, F.; Bazureau, J. P. A stereoselective route to 3-methyl-2-methylsulfanyl-5-yliden-3,4-dihydro-imidazol-4-one derivatives and precursor of Leucettamine B. *Green Chem.* **2001**, *3*, 165–169. (d) Chérouvrier, J. R.; Carreaux, F.; Bazureau, J. P. Microwave-mediated solventless synthesis of new derivatives of marine alkaloid Leucettamine B. *Tetrahedron Lett.* **2002**, *43*, 3581–3584. (e) Debdab, M.; Renault, S.; Eid, S.; Lozach, O.; Meijer, L.; Carreaux, F.; Bazureau, J.-P. An efficient method for the preparation of new analogs of leucettamine B under solvent-free microwave irradiation. *Tetrahedron Let.* **2009**, *78*, 1191–1203.

(13) Hagiwara, M. Alternative splicing: a new drug target of the post-genome era. *Biochim. Biophys. Acta* **2005**, *1754*, 324–331.

(14) (a) Aranda, S.; Laguna, A.; de la Luna, S. DYRK family of protein kinases: evolutionary relationships, biochemical properties, and functional roles. *FASEB J.* **2011**, *25*, 449–462. (b) Kimura, R.; Kamino, K.; Yamamoto, M.; Nuripa, A.; Kida, T.; Kazui, H.; Hashimoto, R.; Tanaka, T.; Kudo, T.; Yamagata, H.; Tabara, Y.; Miki, T.; Akatsu, H.; Kosaka, K.; Funakoshi, E.; Nishitomi, K.; Sakaguchi, G.; Kato, A.; Hattori, H.; Uema, T.; Takeda, M. The DYRK1A gene, encoded in

chromosome 21 Down syndrome critical region, bridges between beta-amyloid production and tau phosphorylation in Alzheimer disease. *Hum. Mol. Genet.* **2007**, *16*, 15–23. (c) Ryoo, S. R.; Jeong, H. K.; Radnaabazar, C.; Yoo, J. J.; Cho, H. J.; Lee, H. W.; Kim, I. S.; Cheon, Y. H.; Ahn, Y. S.; Chung, S. H.; Song, W. J. DYRK1A-mediated hyperphosphorylation of Tau. A functional link between Down syndrome and Alzheimer disease. *J. Biol. Chem.* **2007**, *282*, 34850–34857. (d) Ryoo, S. R.; Cho, H. J.; Lee, H. W.; Jeong, H. K.; Radnaabazar, C.; Kim, Y. S.; Kim, M. J.; Son, M. Y.; Seo, H.; Chung, S. H.; Song, W. J. Dual-specificity tyrosine(Y)-phosphorylation regulated kinase 1A-mediated phosphorylation of amyloid precursor protein: evidence for a functional link between Down syndrome and Alzheimer's disease. *J. Neurochem.* **2008**, *104*, 1333–1344. (e) Ryu, Y. S.; Park, S. Y.; Jung, M. S.; Yoon, S. H.; Kwen, M. Y.; Lee, S. Y.; Choi, S. H.; Radnaabazar, C.; Kim, M. K.; Kim, H.; Kim, K.; Song, W. J.; Chung, S. H. Dyrk1A-mediated phosphorylation of Presenilin 1: a functional link between Down syndrome and Alzheimer's disease. *J. Neurochem.* **2010**, *115*, 574–584. (f) Sitz, J. H.; Baumgärtel, K.; Hämmerle, B.; Papadopoulos, C.; Hekerman, P.; Tejedor, F. J.; Becker, W.; Lutz, B. The Down syndrome candidate dual-specificity tyrosine phosphorylation-regulated kinase 1A phosphorylates the neurodegeneration-related septin 4. *Neuroscience* **2008**, *157*, 596–605. (g) Glatz, D. C.; Rujescu, D.; Tang, Y.; Berendt, F. J.; Hartmann, A. M.; Faltraco, F.; Rosenberg, C.; Hulette, C.; Jellinger, K.; Hampel, H.; Riederer, P.; Möller, H. J.; Andreadis, A.; Henkel, K.; Stamm, S. The alternative splicing of tau exon 10 and its regulatory proteins CLK2 and TRA2-BETA1 changes in sporadic Alzheimer's disease. *J. Neurochem.* **2006**, *96*, 635–644. (h) Wegiel, J.; Kaczmarski, W.; Barua, M.; Kuchna, I.; Nowicki, K.; Wang, K. C.; Wegiel, J.; Yang, S. M.; Frackowiak, J.; Mazur-Kolecka, B.; Silverman, W. P.; Reisberg, B.; Monteiro, I.; de Leon, M.; Wisniewski, T.; Dalton, A.; Lai, F.; Hwang, Y. W.; Adayev, T.; Liu, F.; Iqbal, K.; Iqbal, I. G.; Gong, C. X. Link between DYRK1A overexpression and several-fold enhancement of neurofibrillary degeneration with 3-repeat tau protein in Down syndrome. *J. Neuropathol. Exp. Neurol.* **2011**, *70*, 36–50. (i) Ding, S.; Shi, J.; Qian, W.; Iqbal, K.; Grundke-Iqbal, I.; Gong, C. X.; Liu, F. Regulation of alternative splicing of tau exon 10 by 9G8 and Dyrk1A. *Neurobiol. Aging* **2011** Jan 5. [Epub ahead of print].(j) Liu, F.; Gong, C. X. Tau exon 10 alternative splicing and taupathies. *Mol. Neurodegenertaion* **2008**, *3*,

(15) (a) Wegiel, J.; Dowjat, K.; Kaczmarski, W.; Kuchna, I.; Nowicki, K.; Frackowiak, J.; Mazur Kolecka, B.; Wegiel, J.; Silverman, W. P.; Reisberg, B.; Deleon, M.; Wisniewski, T.; Gong, C. X.; Liu, F.; Adayev, T.; Chen-Hwang, M. C.; Hwang, Y. W. The role of overexpressed DYRK1A protein in the early onset of neurofibrillary degeneration in Down syndrome. *Acta Neuropathol.* **2008**, *116*, 391–407. (b) Park, J.; Oh, Y.; Chung, K. C. Two key genes closely implicated with the neuropathological characteristics in Down syndrome: DYRK1A and RCAN1. *BMB Rep.* **2009**, *42*, 6–15. (c) Shi, J.; Zhang, T.; Zhou, C.; Chohan, M. O.; Gu, X.; Wegiel, J.; Zhou, J.; Hwang, Y. W.; Iqbal, K.; Grundke-Iqbal, I.; Gong, C. X.; Liu, F. Increased dosage of Dyrk1A alters alternative splicing factor (ASF)-regulated alternative splicing of tau in Down syndrome. *J. Biol. Chem.* **2008**, *283*, 28660–28669. (d) Noll, C.; Planque, C.; Ripoll, C.; Guedj, F.; Diez, A.; Ducros, V.; Belin, N.; Duchon, A.; Paul, J. L.; Badel, A.; de Freminville, B.; Grattau, Y.; Bléhaut, H.; Herault, Y.; Janel, N.; Delabar, J. M. DYRK1A, a novel determinant of the methionine-homocysteine cycle in different mouse models over-expressing this Down-syndrome-associated kinase. *PLoS One* **2009**, *4*, e7540.

(16) Roué, N.; Bergman, J. Synthesis of the marine alkaloid leucettamine B. *Tetrahedron* **1999**, *55*, 14729–14738.

(17) (a) Bourgeois, C. F.; Lejeune, F.; Stévenin, J. Broad specificity of SR (serine/arginine) proteins in the regulation of alternative splicing of pre-messenger RNA. *Prog. Nucleic Acid Res. Mol. Biol.* **2004**, *78*, 37–88. (b) Prasad, J.; Colwill, K.; Pawson, T.; Manley, J. L. The protein kinase Clk/Sty directly modulates SR protein activity: both hyper- and hypophosphorylation inhibit splicing. *Mol. Cell. Biol.* **1999**, *19*, 6991–7000.

(18) Fedorov, O.; Huber, K.; Eisenreich, A.; Filippakopoulos, P.; King, O.; Bullock, A. N.; Fabro, D.; Trappe, J.; Rauch, U.; Bracher, F.; Knapp, S. Specific CLK inhibitors from a novel chemotype for regulation of alternative splicing. *Chem. Biol.* **2011**, *18*, 67–76.

(19) Eisenreich, A.; Bogdanov, V. Y.; Zakrzewicz, A.; Pries, A.; Antoniak, S.; Poller, W.; Schultheiss, H. P.; Rauch, U. Cdc2-like kinases and DNA topoisomerase I regulate alternative splicing of tissue factor in human endothelial cells. *Circ. Res.* **2009**, *104*, 589–599.

(20) Muraki, M.; Ohkawara, B.; Hosoya, T.; Onogi, H.; Koizumi, J.; Koizumi, T.; Sumi, K.; Yomoda, J.; Murray, M. V.; Kimura, H.; Furuichi, K.; Shibuya, H.; Krainer, A. R.; Suzuki, M.; Hagiwara, M. Manipulation of alternative splicing by a newly developed inhibitor of Clks. *J. Biol. Chem.* **2004**, *279*, 24246–2454.

(21) Yomoda, J.; Muraki, M.; Kataoka, N.; Hosoya, T.; Suzuki, M.; Hagiwara, M.; Kimura, H. Combination of Clk family kinase and SRp75 modulates alternative splicing of Adenovirus E1A. *Genes Cells* **2008**, *13*, 233–244.

(22) (a) Bain, J.; Plater, L.; Elliott, M.; Shapiro, N.; Hastie, C. J.; McLauchlan, H.; Klevernic, I.; Arthur, J. S.; Alessi, D. R.; Cohen, P. The selectivity of protein kinase inhibitors: a further update. *Biochem. J.* **2007**, *408*, 297–315. (b) Göckler, N; Jofre, G; Papadopoulos, C; Soppa, U; Tejedor, F. J.; Becker, W. Harmine specifically inhibits protein kinase DYRK1A and interferes with neurite formation. *FEBS J.* **2009**, *276*, 6324–6337.

(23) (a) Meijer, L.; Borgne, A.; Mulner, O.; Chong, J. P. J.; Blow, J. J.; Inagaki, N.; Inagaki, M.; Delcros, J. G.; Moulinoux, J. P. Biochemical and cellular effects of roscovitine a potent and selective inhibitor of the cyclin-dependent kinases cdc2 cdk2 and cdk5. *Eur. J. Biochem.* **1997**, *243*, 527–36. (b) Meijer, L.; Raymond, E. Roscovitine and other purines as kinase inhibitors: from starfish oocytes to clinical trials. *Acc. Chem. Res.* **2003**, *36*, 417–425.

(24) Black, D. L. Mechanisms of alternative pre-messenger RNA splicing. *Annu. Rev. Biochem.* **2003**, *72*, 291–336.

(25) Eisenreich, A.; Boltzen, U.; Poller, W.; Schultheiss, H. P.; Rauch, U. Effects of the Cdc2-like kinase-family and DNA topoisomerase I on the alternative splicing of eNOS in TNF-alpha-stimulated human endothelial cells. *Biol. Chem.* **2008**, *389*, 1333–1338.

(26) Nowak, D. G.; Woolard, J.; Amin, E. M.; Konopatskaya, O.; Saleem, M. A.; Churchill, A. J.; Ladomery, M. R.; Harper, S. J.; Bates, D. O. Expression of pro- and anti-angiogenic isoforms of VEGF is differentially regulated by splicing and growth factors. *J. Cell Sci.* **2008**, *121*, 3487–3495.

(27) Leclerc, S.; Garnier, M.; Hoessel, R.; Marko, D.; Bibb, J. A.; Snyder, G. L.; Greengard, P.; Biernat, J.; Mandelkow, E.-M.; Eisenbrand, G.; Meijer, L. Indirubins inhibit glycogen synthase kinase - 3β and CDK5/p25, two kinases involved in abnormal tau phosphorylation in Alzheimer's disease - A property common to most CDK inhibitors ? *J. Biol. Chem.* **2001**, *276*, 251–260.

(28) Primot, A.; Baratte, B.; Gompel, M.; Borgne, A.; Liabeuf, S.; Romette, J. L.; Costantini, F.; Meijer, L. Purification of GSK-3 by affinity chromatography on immobilised axin. *Protein Expression Purif.* **2000**, *20*, 394–404.

(29) Reinhardt, J.; Ferandin, Y.; Meijer, L. Purification CK1 by affinity chromatography on immobilised axin. *Protein Expression Purif.* **2007**, *54*, 101–109.

(30) Leslie, A. G. W.; Powell, H. *MOSFLM*; MRC Laboratory of Molecular Biology: Cambridge, England, 2007.

(31) Evans, P. *SCALA: Scale Together Multiple Observations of Reflections*; MRC Laboratory of Molecular Biology: Cambridge, england, 2007.

(32) Otwinowski, Z.; Minor, W. Processing of X-ray Diffraction Data Collected in Oscillation Mode. *Macromolecular Crystallography, Part A*; Academic Press: New York, 1997; pp 307−326.

(33) McCoy, A. J.; Grosse-Kunstleve, R. W.; Storoni, L. C.; Read, R. J. Likelihood enhanced fast translation functions. *Acta Crystallogr., Sect. D* **2005**, *61*, 458–464.

(34) Bullock, A. N.; Das, S.; Debreczeni, J. E.; Rellos, P.; Fedorov, O.; Niesen, F. H.; Guo, K.; Papagrigoriou, E.; Amos, A. L.; Cho, S.; Turk, B. E.; Ghosh, G.; Knapp, S. Kinase domain insertions define distinct roles of CLK kinases in SR protein phosphorylation. *Structure* **2009**, *17*, 352–362.

(35) Perrakis, A.; Morris, R.; Lamzin, V. S. Automated protein model building combined with iterative structure refinement. *Nat. Struct. Biol.* **1999**, *6*, 458–463.

(36) Emsley, P.; Cowtan, K. Coot: model-building tools for molecular graphics. *Acta Crystallogr., Sect. D* **2004**, *60*, 2126–2132.
(37) Murshudov, G. N.; Vagin, A. A.; Dodson, E. J. Refinement of macromolecular structures by the maximum-likelihood method. *Acta Crystallogr., Sect. D* **1997**, *53*, 240–255.
(38) Szotowski, B.; Goldin-Lang, P.; Antoniak, S.; Bogdanov, V. Y.; Pathirana, D.; Pauschinger, M.; Dörner, A.; Kuehl, U.; Coupland, S.; Nemerson, Y.; Hummel, M.; Poller, W.; Hetzer, R.; Schultheiss, H. P.; Rauch, U. Alterations in myocardial tissue factor expression and cellular localization in dilated cardiomyopathy. *J. Am. Coll. Cardiol.* **2005**, *45*, 1081–1089.
(39) Hernández, F.; Gómez de Barreda, E.; Fuster-Matanzo, A.; Lucas, J. J.; Avila, J. GSK3: a possible link between beta amyloid peptide and tau protein. *Exp. Neurol.* **2010**, *223*, 322–325.